Diamond & Related Materials 151 (2025) 111796

Contents lists available at ScienceDirect

Diamond & Related Materials

journal homepage: www.elsevier.com/locate/diamond

Rheological modeling of MWCNT-Al_2O_3 hybrid nanofluid using cascade forward neural network method

Mohammad Javad Kholoud [a], Noushin Mahmoudi Soumar [b], Amin Torabi [c], Mehdi Jamali Ghahderijani [a,d], Mohammd Hossein Razavi Dehkordi [a,d,*]

[a] Department of Mechanical Engineering, Najafabad Branch, Islamic Azad University, Najafabad, Iran
[b] Department of Chemical Engineering, Shahreza Branch, Islamic Azad University, Shahreza, Iran
[c] Aerospace PHD Graduated, Aerospace Engineering Department, Sharif University of Technology, Tehran, Iran
[d] Aerospace and Energy Conversion Research Center, Najafabad Branch, Islamic Azad University, Najafabad, Iran

ARTICLE INFO

Keywords:
Artificial intelligence
Cascade forward neural network (CFNN)
Viscosity modeling
Levenberg-Marquardt algorithm

ABSTRACT

Hybrid nanofluids have gained popularity in recent years due to their unique thermal properties. This study investigates the rheological behavior of an MWCNT-Al_2O_3 hybrid nanofluid as a coolant in thermal cycles using artificial intelligence (AI) analysis. Viscosity measurements were taken across varying solid concentrations, temperatures, and shear rates, ranging from 0.25 % to 1 % solid concentration, 25 °C to 50 °C temperature, and 20 to 60 RPM shear rate. Employing a Cascade Forward Neural Network (CFNN) with two hidden layers, alongside the Levenberg-Marquardt algorithm for training, the study models viscosity across these independent variables' ranges. The results indicate that the CFNN captures a substantial portion of data variability, providing a good fit to observed data points. The regression lines with R-squared values of 0.999 and 0.997 for the training and test phases indicate that the fit is almost ideal. Also, the maximum absolute error of 0.4992 show that the error values are acceptable. Furthermore, the trained CFNN effectively estimates viscosity at any desired combination of independent variables, demonstrating stable performance across different runs and data subsets.

1. Introduction

Hybrid nanofluids, which consist of multiple types of nanoparticles suspended in a base fluid, have gained significant attention due to their enhanced thermal properties and potential for improving heat transfer in applications such as cooling systems. However, accurately predicting their rheological behavior under varying conditions of solid concentration, temperature, and shear rate remains challenging. AI and machine learning (ML) offer powerful solutions for modeling these complex behaviors. ML techniques have shown promise in a variety of engineering fields. For example, ML algorithms for vehicle-railway bridge collision detection and overheight vehicle warning [1,2], statistical machine learning models for optimizing energy in industrial application [3,4], image processing for identifying vehicles and traffic monitoring [5,6]. In the context of nanofluid rheology, AI-based methods like Cascade Forward Neural Networks (CFNN) can effectively model the complex relationships between viscosity and variables like nanoparticle concentration, temperature, and shear rate. Previous studies have also applied numerical models to analyze nanofluid convection and heat transfer in different geometries [7,8], but predictive modeling using AI remains less explored. Also, the rheological behavior of fluids can be complex, and it is often difficult to predict how a fluid will behave under certain conditions. This is especially true for hybrid nanofluids, which are suspensions of nanoparticles in a base fluid [9]. The properties of hybrid nanofluids can vary significantly depending on the type of nanoparticles used, the concentration of nanoparticles, and the size and shape of the nanoparticles. As a result, it is important to have a good understanding of the rheological behavior of hybrid nanofluids in order to use them effectively in industrial applications. Viscosity is a key parameter in the study of the rheological behavior of fluids. It is a measure of the resistance of a fluid to flow and is defined as the ratio of the shear stress to the rate of shear strain. The viscosity of a fluid can be affected by a number of factors, including temperature, pressure, and the presence of suspended particles [10,11]. One of the most promising methods for studying the rheological behavior of hybrid nanofluids is artificial neural networks (ANNs) [12]. ANNs are powerful machine learning tools that can be used to model complex relationships between inputs and outputs [13]. In the case of hybrid nanofluids, ANNs can be

* Corresponding author at: Department of Mechanical Engineering, Najafabad Branch, Islamic Azad University, Najafabad, Iran.
E-mail address: mohammadhossainrazavi@gmail.com (M.H.R. Dehkordi).

https://doi.org/10.1016/j.diamond.2024.111796
Received 17 September 2024; Received in revised form 10 November 2024; Accepted 16 November 2024
Available online 17 November 2024

used to model the relationship between the rheological properties of the fluid and the various parameters that affect them. This information can then be used to design hybrid nanofluids with specific rheological properties for specific applications [14,15]. Some previous studies investigate the use of numerical methods to predict the rheological behavior of nanofluids. Using ANN and Response Surface Methodology (RSM) methods, Hemmat et al. [16] investigated the thermophysical properties of CNT nanofluid based on water-ethylene glycol (EG) mixture including viscosity, thermal conductivity and specific heat. Their results showed that both ANN and RSM models have good ability to predict parameters, but multilayer perceptron (MLP) was more accurate than RSM in predicting relative viscosity. Also, the results of optimization with NSGA-II algorithm for different conditions showed that these points do not have priority over each other and all are optimal. Mahfouz et al. [17] have utilized RSM to develop a prediction model for the viscosity of a TiO_2 nanotube nanofluid in an EG-water solution. They have explored various mass concentrations (0 % to 1 %), shear rates (150–500 s^{-1}), and temperatures (25 to 65 °C). Optimization studies have revealed nanofluid concentration as the most influential parameter, followed by temperature and shear rate. Case studies have demonstrated optimal conditions for both viscosity maximization and minimization. Ajuka et al. [18] have examined the viscosity of TiO2-Al2O3/EG composite nanofluid using both experimental correlation and ANN methods. They have utilized 15 and 13 nm nominal surface-area weighted diameter TiO2 and Al2O3 nanoparticles to formulate nanofluids at various volume fractions. A theoretical correlation and ANN model have been developed to predict viscosity dependence on volume fraction and temperature. Both methods have exhibited high predictive ability with minimal relative error compared to experimental results. Nayebpashaee and Hadavi [19] investigates nanoparticle concentration and temperature's effect on thermophysical properties of graphene-Al2O3/EG-water nanofluid. Their outcomes demonstrated viscosity increases with nanoparticles, exhibiting non-Newtonian behavior at higher concentrations. They proposed a correlation for thermal conductivity assessment. Yashawantha et al. [20] investigated graphite-EG nanofluid's rheological behavior and thermal conductivity. Viscosity and thermal conductivity are studied across various conditions, revealing viscosity increases with concentration but decreases with temperature, while thermal conductivity notably enhances with 2 % volume concentration and nanoparticle size below 50 nm. Kumar et al. [21] investigated the temperature-dependent thermophysical properties of various hybrid nanofluids. They utilize MWCNT-water-based Al_2O_3, TiO_2, ZnO, and CeO_2 nanofluids, mixing them in an 80:20 volumetric ratios. Nanofluids were prepared with concentrations ranging from 0.25 % to 2.0 % and tested at temperatures from 25 °C to 50 °C. CeO_2-MWCNT/water nanofluid exhibited superior efficacy. An optimized ANN model accurately predicted properties across four thermophysical parameters. The ANN achieved high accuracy compared to experimental results. Long Li et al. [22] investigated the stability and thermophysical properties of Al_2O_3-EG nanofluids. Their research aimed to assess stability through nanoparticle size and velocity ratio analysis, while evaluating heat transfer performance using various criteria. They utilized correlations and an ANN model to predict viscosity and thermal conductivity. Notably, their findings, particularly regarding nanofluids treated for 60 min, offer valuable insights for nanofluid stability studies and practical applications. Akhgar et al. [23] introduced dissimilar ANNs for predicting MWCNT-TiO_2/Water-EG nanofluid thermal conductivity. Sensitivity analysis informs ANN architecture and training algorithms. The ANN forecasts conductivity based on temperature and concentration changes, outperforming correlations. MWCNTs-TiO_2 hybrid nanoparticles are used at a 50:50 volume ratio. Their results showed ANN's superior prediction capability over correlations.

Until now, a variety of machine learning algorithms are applied for the prediction of nanofluid properties. For example, GMDH-NN and COMBI algorithms are used by [24], Gaussian process regression (GPR) is utilized by [25,26], and Adaptive Neuro-Fuzzy Inference System (ANFIS) is employed by [26,27]. The Cascade-Forward Neural Networks (CFNN) is a powerful machine learning algorithm for the prediction and regression purposes. The use of the CFNN is appropriate for small datasets with complex relationships between inputs and targets due to the capability for maximum information utilization. Despite suitable performance, the CFNN has very limited application in the prediction of nanofluid properties. This research pioneers the use of the CFNN to develop a predictive model for nanofluid viscosity, as demonstrated in the work of Afshari et al. [28]. Moreover, this study explores a specific hybrid nanofluid, filling a significant gap in nanofluid research that has been largely neglected in previous investigations. By scrutinizing viscosity under various conditions—temperature, shear rate, and volume fraction—the study unveils a remarkably precise model for dynamic viscosity assessment. Offering invaluable insights, this paper paves the way for future advancements in nanofluid exploration and development.

Table 1
Specifications of MWCNTs and Al_2O_3 nanoparticles [28].

Specifications	Value	
	Al_2O_3	MWCNTs
Purity (%)		97
Color	White	Black
Size (nm)	20	Outer Diameter = 5–15 Inner Diameter = 3–5 Length = 50
Thermal conductivity ($W\,m-1\,k-1$)	30	1500
Density ($g\,cm-3$)	3.89	2.1
Specific surface ($m2\,g-1$)	138	233

Table 2
Specifications of water and EG [28].

Specifications	Value	
	EG	Water
Molar mass ($g\,mol-1$)	62.07	18.02
Appearance	Colorless transparent liquid	Almost colorless transparent
Smell	Smell-less	Smell-less
Density ($kg\,m-3$)	1113.20	998.21
Melting point (°C)	−12.9	0.00
Boiling point (°C)	197.3	100
Thermal conductivity ($W\,m-1\,k-1$)	0.224 in 20 °C	0.6 in 20 °C
Viscosity	16.1 in 20 °C	1 in 20 °C

2. The dataset

Afshari et al. [28] employed a two-stage method to prepare nanofluid. Initially, they synthesized Al_2O_3 in a blend of Water (80 %) and EG (20 %) at concentrations ranging from 0.0625 % to 1 % by mixing dry samples of MWCNTs and Al2O3 nanoparticles (in a 50:50 ratio) with a specific quantity of the Water and EG dual mixture (20:80). Tables 1 and 2 detail the specifications of MWCNTs and Al_2O_3 nanoparticles, as well as the specifications of the Water and EG components used in the experiments. This nanofluid, comprising MWCNTs, Al_2O3 nanoparticles, and Water-EG, was then introduced into a 600 ml beaker. The dynamic viscosity of the hybrid nanofluid was measured using the DV-I PRIME Brookfield digital viscometer, featuring a double-wall cylindrical container. Temperature variations of 25, 30, 35, 40, 45, and 50 °C were utilized in their study.

In this study, 120 experiments were done in the Ashari's study [28] to estimate the viscosity of the hybrid nanofluid of MWCNT–alumina/water (80 %)–EG (20 %) which were shown in Table 3. The concentration, temperature and shear rate served as the independent variables, while the viscosity was considered as the dependent variable. In this

Table 3
The used experimental tests as independent and dependent variables for cascade-forward neural network [28].

Independent variables			Dependent variable	Independent variables			Dependent variable
Solid concentration	Temperature	Shear Rate	Viscosity	Solid concentration	Temperature	Shear Rate	Viscosity
0.25	25	20	1.92	0.75	25	5	10.06
0.25	25	30	1.92	0.75	25	10	7.84
0.25	25	40	1.9	0.75	25	20	6.51
0.25	25	50	1.87	0.75	25	30	5.67
0.25	25	60	1.84	0.75	25	40	5.2
0.25	30	20	1.79	0.75	30	5	9.23
0.25	30	30	1.79	0.75	30	10	6.79
0.25	30	40	1.75	0.75	30	20	5.82
0.25	30	50	1.74	0.75	30	30	4.96
0.25	30	60	1.71	0.75	30	40	4.66
0.25	35	20	1.68	0.75	35	5	7.81
0.25	35	30	1.64	0.75	35	10	6.28
0.25	35	40	1.62	0.75	35	20	5.06
0.25	35	50	1.58	0.75	35	30	4.15
0.25	35	60	1.56	0.75	35	40	3.86
0.25	40	20	1.51	0.75	40	5	6.9
0.25	40	30	1.5	0.75	40	10	5.37
0.25	40	40	1.49	0.75	40	20	4.29
0.25	40	50	1.45	0.75	40	30	3.56
0.25	40	60	1.42	0.75	40	40	3.18
0.25	45	20	1.48	0.75	45	5	6.25
0.25	45	30	1.45	0.75	45	10	5.13
0.25	45	40	1.43	0.75	45	20	3.87
0.25	45	50	1.4	0.75	45	30	3.26
0.25	45	60	1.37	0.75	45	40	2.87
0.25	50	20	1.39	0.75	50	5	5.21
0.25	50	30	1.37	0.75	50	10	4.29
0.25	50	40	1.35	0.75	50	20	3.3
0.25	50	50	1.33	0.75	50	30	2.82
0.25	50	60	1.3	0.75	50	40	2.55
0.5	25	20	2.69	1	25	5	19.67
0.5	25	30	2.66	1	25	10	14.21
0.5	25	40	2.62	1	25	15	11.15
0.5	25	50	2.58	1	25	20	9.68
0.5	25	60	2.53	1	25	25	8.95
0.5	30	20	2.39	1	30	5	18.92
0.5	30	30	2.39	1	30	10	13.65
0.5	30	40	2.33	1	30	15	10.82
0.5	30	50	2.32	1	30	20	9.33
0.5	30	60	2.28	1	30	25	8.36
0.5	35	20	2.25	1	35	5	17.18
0.5	35	30	2.2	1	35	10	12.18
0.5	35	40	2.17	1	35	15	9.51
0.5	35	50	2.12	1	35	20	8.11
0.5	35	60	2.08	1	35	25	7.48
0.5	40	20	1.97	1	40	5	16.36
0.5	40	30	1.96	1	40	10	10.93
0.5	40	40	1.95	1	40	15	8.59
0.5	40	50	1.9	1	40	20	7.76
0.5	40	60	1.85	1	40	25	7.02
0.5	45	20	1.87	1	45	5	14.5
0.5	45	30	1.85	1	45	10	10.31
0.5	45	40	1.83	1	45	15	7.98
0.5	45	50	1.8	1	45	20	7.16
0.5	45	60	1.75	1	45	25	6.54
0.5	50	20	1.81	1	50	5	13.22
0.5	50	30	1.79	1	50	10	9.96
0.5	50	40	1.76	1	50	15	7.78
0.5	50	50	1.74	1	50	20	7
0.5	50	60	1.7	1	50	25	6.44

paper, the experimental tests at solid concentrations of 0.25, 0.5, 0.75, and 1 %, the temperatures of 25, 30, 35, 40, 45, and 50 °C, and the shear rates of 5 to 60 RPM were used. The primary goal of the research was to estimate the viscosity of the hybrid nanofluid based on the available data for any desired combination of independent variables within the examined ranges.

3. The cascade-forward neural network

The use of accurate data and method are very vital in performing machine learning and the importance of this issue has been proven in previous research [29]. In comparison to the findings previous study [30], which utilized an ANN approach to predict the thermophysical properties of MWCNT nanofluids, this study employs a cascade forward neural network for the rheological modeling of MWCNT-Al_2O_3 hybrid nanofluids, thereby offering new insights into the combined effects of these hybrid materials on fluid behavior. A CFNN is a variant of the traditional feed-forward neural network. In this modified architecture, each layer of neurons not only receives input from its previous layer but also directly from the input layer and all hidden layers. The network

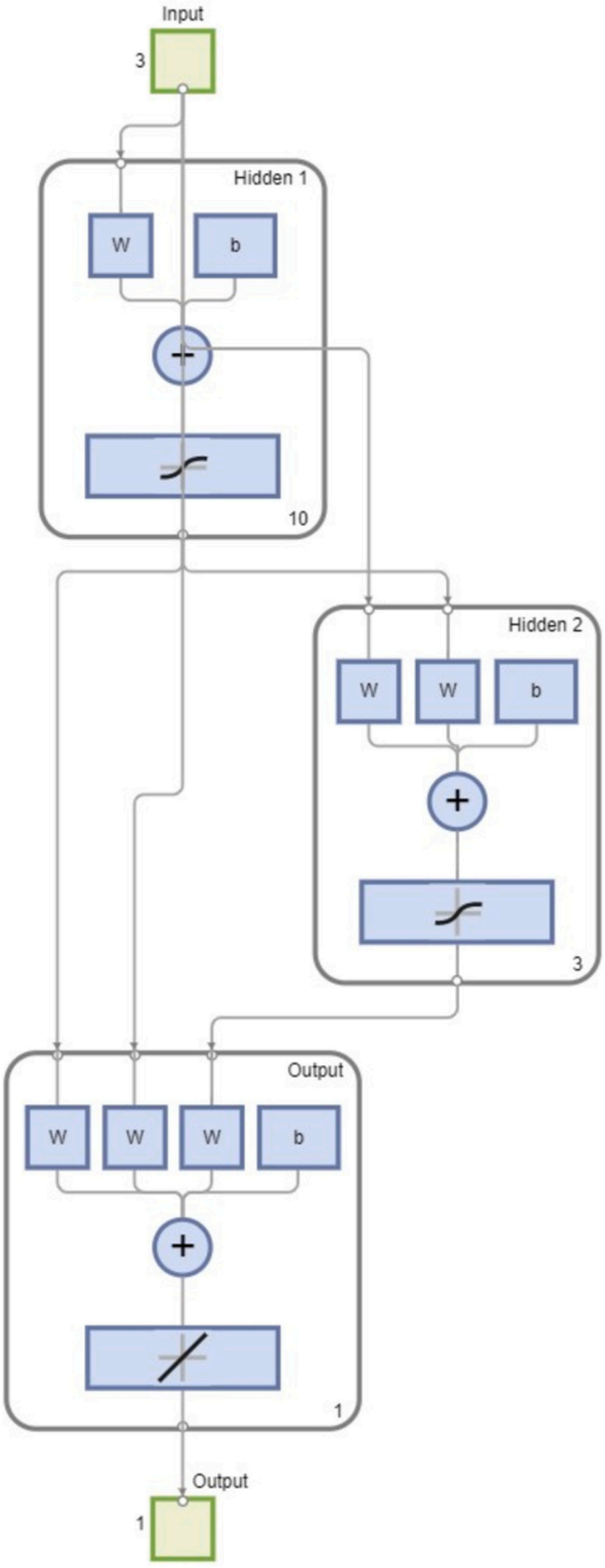

Fig. 1. The architecture of the employed CFNN.

starts with an input layer which is connected to all hidden layer. The hidden layers receive input from other hidden layers and the input layer. Also, the output layer receives input from all hidden layers, as well as from the input layer. This means that each neuron in a layer is connected to all neurons in the previous layer as well as the input layer. By incorporating more connectivity, the CFNN enables each neuron to consider information from all preceding layers, enhancing its ability to capture complex relationships in the data. This results in improved representation learning and increased model capacity, making the network more effective at extracting informative features and learning intricate patterns in the data. Additionally, the connections contribute to the network's robustness to input variations, leading to improved generalization performance on unseen data. Therefore, CFNN can potentially enhance the network's ability to learn complex patterns and relationships in the data by providing more comprehensive information to each layer.

While the CFNN offers several advantages, it also has some potential disadvantages. One drawback is increased computational complexity due to the connectivity pattern, which results in a higher number of parameters and computational requirements compared to networks with sparser connections. This increased complexity can lead to longer training times and higher memory usage, particularly for large-scale datasets and complex architectures.

The use of the CFNN is suitable for small datasets with complex relationships between inputs and targets due to its capacity for enhanced information flow. This design ensures that each layer receives direct input not only from the previous layer but also from the input layer, allowing the network to efficiently leverage available information. In scenarios with limited data, this connectivity pattern helps prevent overfitting by focusing on essential features and reducing the risk of memorizing noise. Additionally, the straightforward flow of information from input to output facilitates effective learning of complex relationships, enabling the network to achieve robust performance despite the dataset's size constraints. Thus, this architecture offers a balanced approach that maximizes information utilization while addressing the challenges of small datasets, making it well-suited for tasks requiring the modeling of intricate relationships with limited data where robust performance on unseen data is crucial. Due to these features, the CFNN is an optimal choice for this paper.

4. The network features

Data division in neural networks serves crucial purposes. It enables training the model on one portion of the dataset to learn patterns and optimize parameters. Another segment is reserved for validation, facilitating hyperparameter tuning and preventing overfitting. The remaining portion, the test set, allows an unbiased evaluation of the model's performance on unseen data, ensuring its effectiveness in real-world applications. In this paper data is divided randomly to the training, validation and test datasets. The training, validation and test datasets ratios are selected 0.7, 0.15, and 0.15, respectively.

The selection of the optimal number of hidden layers and neurons in a neural network involves specifying an initial architecture. This baseline is then iteratively adjusted by varying the number of hidden layers and neurons, and the model's performance is evaluated on a validation dataset. Through comparative analysis, the architecture demonstrating superior performance is selected. The process includes refining the search space based on insights gained and ensuring the robustness and reproducibility of results. In this paper, a CFNN with two hidden layers is selected. The number of hidden neurons are 10 and 3, respectively. The architecture of the employed CFNN is illustrated in Fig. 1.

For the first hidden layer, the mathematical expression is as follows:

$$h^{(1)} = \sigma\left(W^{(1-0)}x + b^{(1)}\right) \tag{1}$$

Table 4
The summarized details of the employed ANN.

Feature	Value
ANN type	CFNN
Number of hidden layers	2
Number of hidden neurons	10, 3
Number of input features	3
Number of output features	1
The activation function	sigmoid
The training datasets ratios	0.7
The validation datasets ratios	0.15
The test datasets ratios	0.15
training algorithm	Levenberg-Marquardt

where $W^{(1-0)}$ is a 10 × 3 matrix (10 hidden neurons, 3 input features), and $b^{(1)}$ is a 10 × 1 bias vector. Also, σ represents the sigmoid activation function.

For the second hidden layer, the mathematical expression is as follows:

$$h^{(2)} = \sigma\left(W^{(2-0)}x + W^{(2-1)}h^{(1)} + b^{(2)}\right) \quad (2)$$

where $W^{(2-0)}$ is a 3× 3 matrix (3 hidden neurons, 3 input features), $W^{(2-1)}$ is a 3 × 10 matrix (3 hidden neurons, 10 inputs from the first hidden layer), and $b^{(2)}$ is a 3 × 1 bias vector. Finally, for the output layer, the mathematical expression is as follows:

$$y = W^{(3-0)}x + W^{(3-2)}h^{(2)} + b^{(3)} \quad (3)$$

where $W^{(3-0)}$ is a 1 × 3 matrix (1 output neuron, 3 input features), $W^{(3-2)}$ is a 1× 3 matrix (1 output neuron, 3 inputs from the second hidden layer), and b(3) is a 1 × 1 bias vector.

The process of selecting the best training algorithm for a neural network involves choosing candidate algorithms based on literature or empirical experimentation, implementing and training models using each algorithm, evaluating performance on a validation dataset, comparing results, and identifying algorithms with superior performance. In this paper, Levenberg-Marquardt algorithm is identified as the optimal training algorithm. The Levenberg-Marquardt algorithm offers several advantages when dealing with small datasets, primarily due to its faster convergence and efficiency in optimizing nonlinear problems. It combines the benefits of gradient descent and the Gauss-Newton method, allowing for quicker training times and requiring less computational overhead per iteration. Additionally, it provides direct control over the trade-off between fitting the training data and maintaining model simplicity through its damping parameter, which helps prevent overfitting—a common issue with small datasets.

The details of the employed ANN are summarized in Table 4.

5. Results

A performance plot, or learning curve, visualizes the CFNN model's accuracy over training epochs. It typically comprises training, validation, and test plots, illustrating the model's learning process, generalization ability to unseen data, and final performance. The training plot shows the model's performance on the training dataset, while the validation plot indicates its generalization to a separate validation dataset. The test plot evaluates the model's performance on unseen data after training. Analyzing these plots provides insights into the model's learning dynamics, generalization, and real-world effectiveness. In this paper, the Mean Squared Error (MSE) is selected as the performance criterion. The MSE is defined as follows [31]:

$$MSE = \frac{1}{m}\sum_{i=1}^{m}(y_i - t_i)^2 \quad (4)$$

In which y is the estimated output, t is the targets, and m shows the number of samples.

The performance plot is illustrated in Fig. 2. As can be seen for the training curve, the MSE is decreasing throughout the learning process. For the validation dataset, however, the MSE decreases initially and then increases. The best performance for the validation dataset is 0.0626 obtained at epoch 21. To prevent over-fitting, the training process is halted 6 iterations after the best performance. The test curve is very similar to the validation dataset. Based on the results, the learning process demonstrates excellent performance.

A regression plot visualizes the relationship between predicted and actual values in a regression model. In training plots, predicted values from the model are compared to actual target values in the training

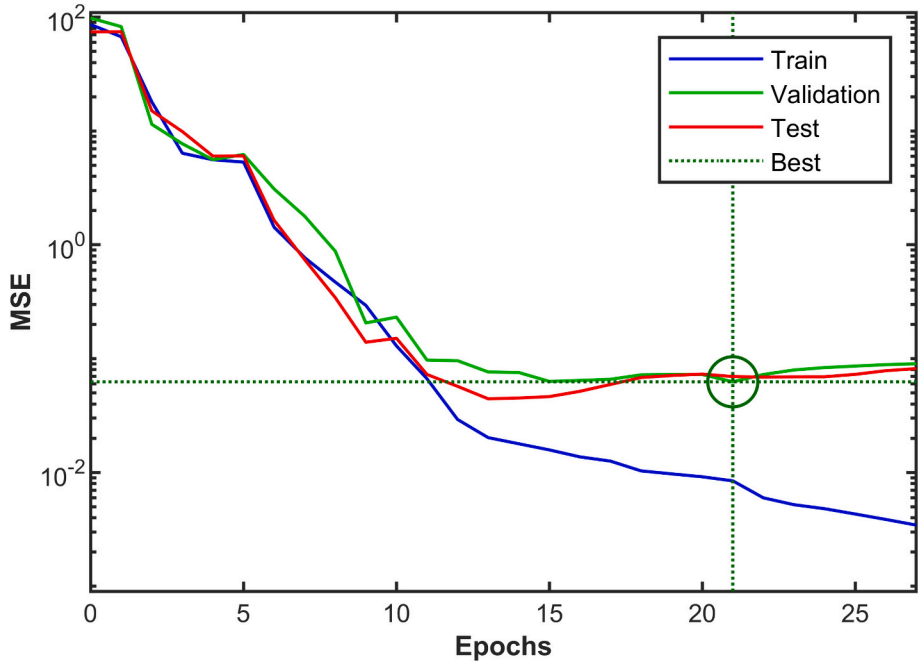

Fig. 2. The performance plot.

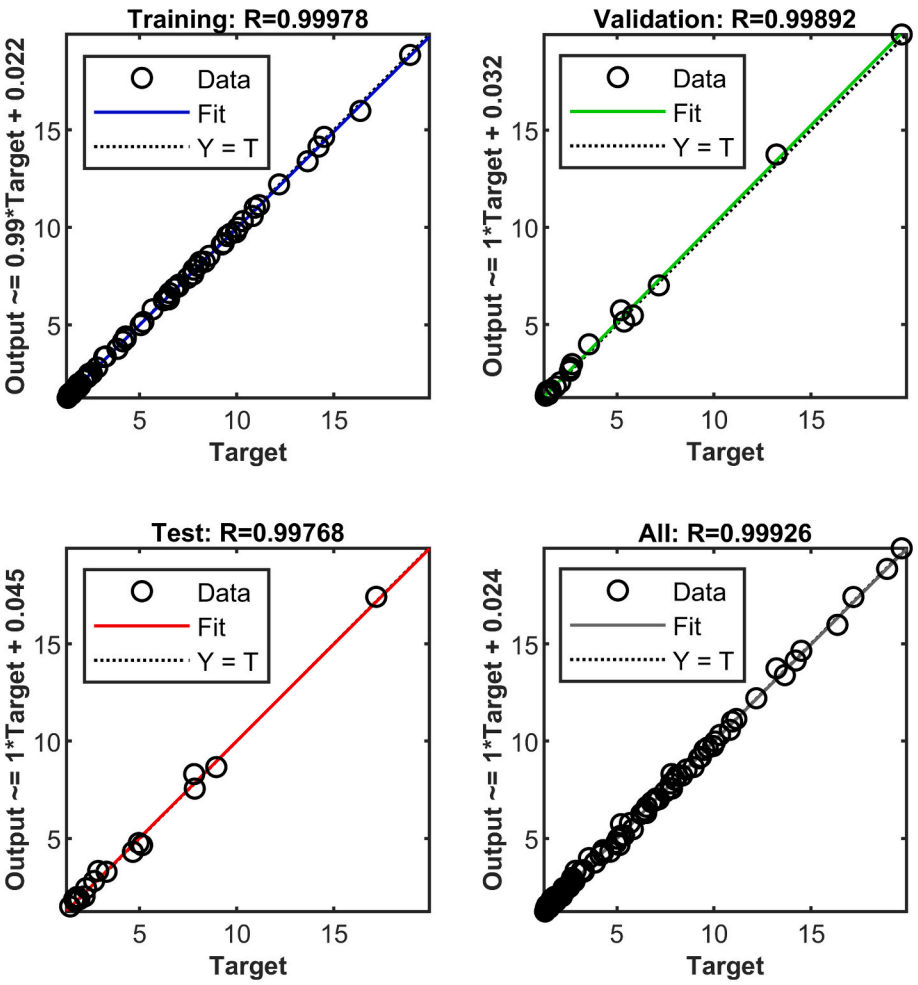

Fig. 3. The regression plot.

dataset, showing how well the model fits the training data. Validation plots depict this relationship using a separate validation dataset, evaluating the model's generalization performance. Test plots extend this evaluation to unseen data in a separate test dataset. These plots aid in assessing the accuracy and generalization ability of the model by visually comparing predicted values to actual targets across different datasets.

In a regression plot, the slope, bias, and R-squared (R^2) values serve as important indicators of the model's performance and the relationship between the predictor and target variables. The R^2 is defined as follows [32,33]:

$$R^2 = 1 - \sum_{i=1}^{m} \frac{(y_i - t_i)^2}{(\bar{t} - t_i)^2} \tag{5}$$

In which y is the estimated output, t is the targets, $\bar{t}$ is the average of targets, and m shows the number of samples.

An ideal scenario often involves a slope close to 1, indicating that the predicted variable changes in tandem with the predictor variable. This suggests a strong linear relationship between the variables, which is desirable in many regression analyses. Additionally, a bias value that approaches zero is typically preferred. A vanishing bias suggests that the predicted variable is close to the true value when the predictor variable is zero, indicating minimal systematic error or constant offset in the model's predictions. Furthermore, an R-squared value near 1 signifies a high proportion of the variance in the dependent variable that is explained by the independent variables. This indicates that the regression model captures a significant portion of the variability in the data

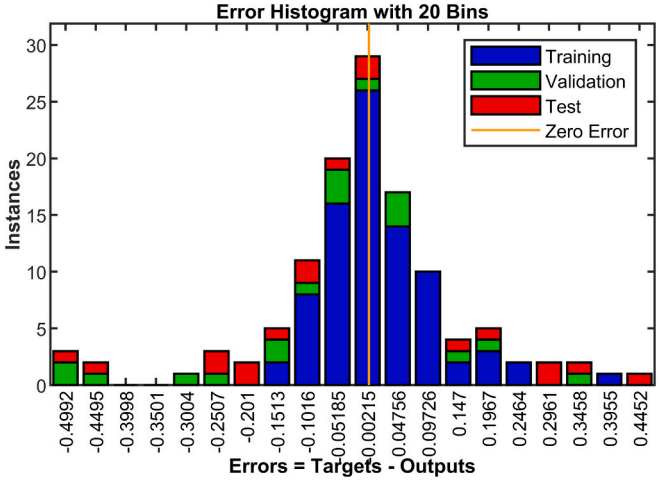

Fig. 4. The error histogram.

and provides a good fit to the observed data points. The regression plot is shown in Fig. 3. As can be seen, the regressions are almost ideal.

An error histogram is a graphical representation that illustrates the distribution of errors in a dataset. The errors typically represent the discrepancies between the predicted values generated by the model and the actual observed values. The histogram visually displays the frequency or count of these errors across different bins. The error histogram

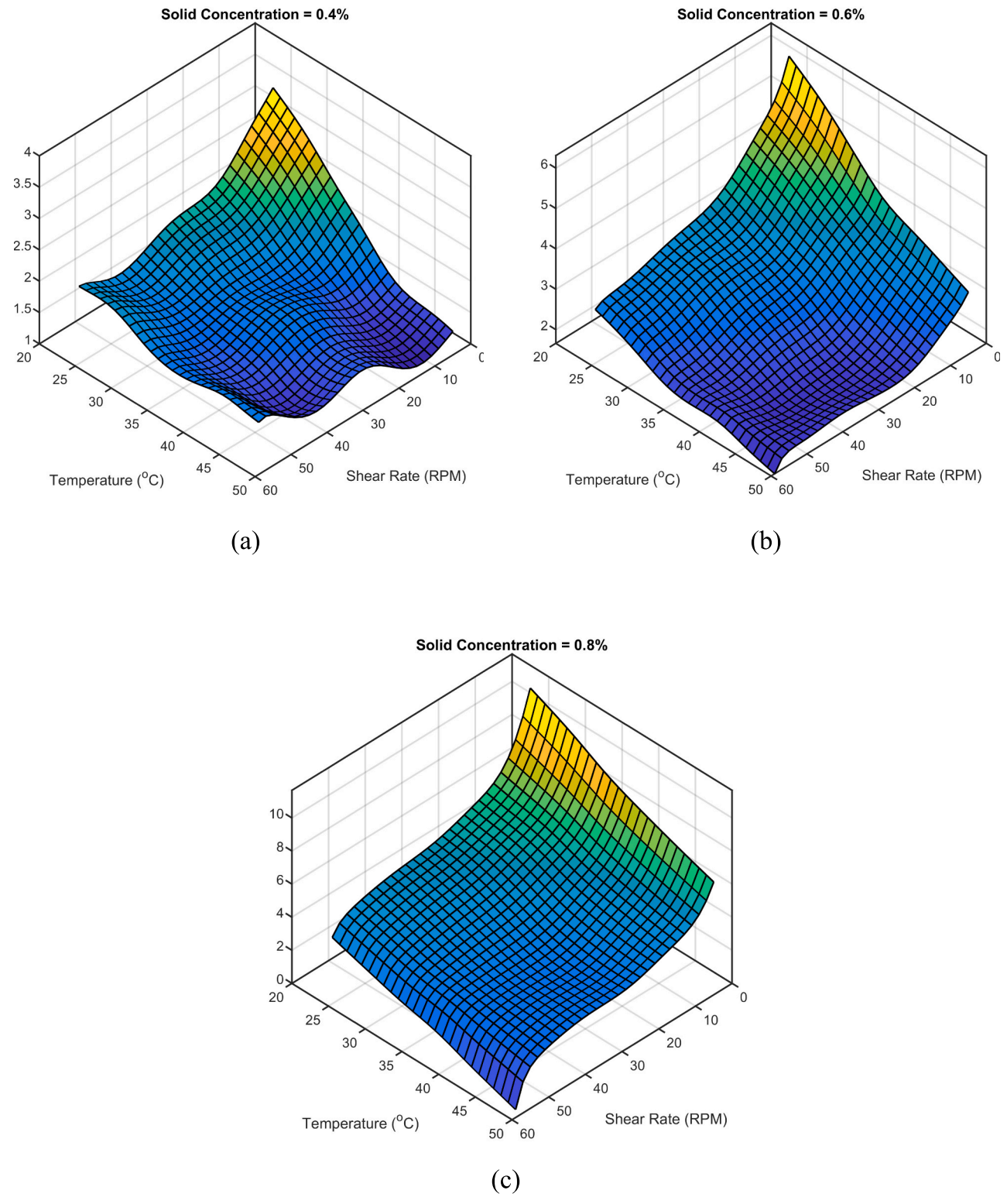

Fig. 5. The viscosity estimated by the CFNN for the solid concentrations of (a) 0.4 %, (b) 0.6 %, and (c) 0.8 %.

shows the distribution of prediction errors, identify any patterns or trends, and assess the overall accuracy and performance of the predictive model. The error histogram is shown in Fig. 4. The symmetrical, normal distribution of errors around zero indicates unbiased predictions. Also, the narrow spread with most errors concentrated near zero, suggesting accurate and consistent predictions. Furthermore, there are few outliers or extreme errors, and the histogram shows consistent distributions across different bins or ranges. A lack of systematic patterns or biases indicates a well-performing model.

The trained CFNN is able to estimate the viscosity at any desired combination of independent variables. The viscosity estimated by the CFNN for 3 non-trained solid concentrations are shown in Fig. 5. Evaluating the model's output for acceptable generalization involves examining its performance on a dataset that it hasn't been trained on provides insights into how well the model can generalize to unseen data. Based on the results, stable performance across different runs or data subsets can

be seen. Also, validation against expert judgment ensures that the model's predictions align with expectations and make intuitive sense. Therefore, one can ascertain the model ability to generalize effectively and perform well on unseen data, contributing to its overall reliability and effectiveness in real-world applications.

6. Conclusion

In conclusion, this study has successfully explored the viscosity of MWCNT-Al_2O_3 hybrid nanofluid across a range of volume fractions, temperatures, and shear rates. Utilizing a CFNN with two hidden layers, trained with the Levenberg-Marquardt algorithm, proved effective in modeling viscosity variations within the investigated parameter ranges. The results demonstrate the network's capability to capture a significant portion of data variability, providing a good fit to observed data points. Notably, observed physical phenomena such as the increase in viscosity with higher volume fractions, which aligns with findings from previous studies [28,34]. This behavior can be attributed to the higher concentration of nanoparticles leading to increased particle-particle interactions and aggregate formation. Conversely, the decrease in viscosity with rising temperatures is consistent with the behavior of conventional fluids. This can be explained by the reduction in intermolecular forces at elevated temperatures, which enhances the fluid's flow characteristics. Additionally, the results indicate that increasing the shear rate and temperature decreases viscosity, reflecting the behavior of shear-thinning fluids. This reduction is due to the diminishing resistance against shear forces and the enhanced momentum transfer in the nanofluids. Moreover, the trained CFNN exhibited stable performance across different runs and data subsets, showcasing its reliability in estimating viscosity at any desired combination of independent variables. This robustness is crucial for practical applications, as it indicates that the model can reliably predict viscosity under varying operational conditions. This comprehensive analysis contributes valuable insights into understanding and predicting the viscosity behavior of hybrid nanofluids, thus advancing knowledge in this field. The findings suggest that optimizing the use of these hybrid nanofluids could significantly enhance the efficiency of thermo-fluid systems, offering potential benefits in various engineering applications, such as heat exchangers and cooling systems.

CRediT authorship contribution statement

Mohammad Javad Kholoud: Writing – original draft, Data curation, Conceptualization. **Noushin Mahmoudi Soumar:** Writing – original draft, Investigation, Formal analysis. **Amin Torabi:** Writing – original draft, Methodology, Investigation. **Mehdi Jamali Ghahderijani:** Validation, Software. **Mohammd Hossein Razavi Dehkordi:** Supervision, Resources, Methodology, Conceptualization.

Declaration of competing interest

The authors declare that they have no known competing financial interests or personal relationships that could have appeared to influence the work reported in this paper.

Data availability

Data will be made available on request.

References

[1] K. Hallak, A. Abdallah, A supervised machine learning monitoring system for vehicle-railway bridge collision, Artificial Intelligence and Applications 2 (4) (2024) 343–357, 10/28.

[2] O. Trembearth, Q. Sun, S. Wang, M. Duckham, Spatial digital twin framework for overheight vehicle warning and re-routing system, Urban Informatics 3 (1) (2024) 23, 07/25, 2024.

[3] C. Zhang, X. Zhang, X. Wu, S. Aziz, Statistical machine learning model for distributed energy planning in industrial park, Artificial Intelligence and Applications 2 (4) (2024) 309–322, 10/28.

[4] X. Fu, Statistical machine learning model for capacitor planning considering uncertainties in photovoltaic power, Protection and Control of Modern Power Systems 7 (1) (2022) 1–13.

[5] E.V. Butilă, R.G. Boboc, Urban traffic monitoring and analysis using unmanned aerial vehicles (UAVs): a systematic literature review, Remote Sens. 14 (2022).

[6] M. Hasanvand, M. Nooshyar, E. Moharamkhani, and A. Selyari, "Machine learning methodology for identifying vehicles using image processing," Artificial Intelligence and Applications, vol. 1, no. 3, pp. 170–178, 04/19, 2023.

[7] M. Mahmoodi, A.A.A. Abbasian, S.S. Mazrouei, S. Nazari, M. Akbari, Free convection of a nanofluid in a square cavity with a heat source on the bottom wall and partially cooled from sides, Therm. Sci. 18 (Suppl. 2) (2014) 283–300.

[8] M. Hemmat Esfe, A. Zare Ghadi, S. Mirtalebi Esforjani, M. Akbari, Combined convection in a lid-driven cavity with an inside obstacle subjected to Al_2O_3-water nanofluid: effect of solid volume fraction and nanofluid variable properties, Acta Phys. Pol. A 124 (4) (2013) 665–672.

[9] N. Azimy, M.R. Saffarian, A. Noghrehabadi, Thermal performance analysis of a flat-plate solar heater with zigzag-shaped pipe using fly ash-Cu hybrid nanofluid: CFD approach, Environ. Sci. Pollut. Res. 31 (12) (2022) 18100–18118.

[10] H. Azimy, A.H. Meghdadi Isfahani, M. Farahnakian, Investigation of the effect of ultrasonic waves on heat transfer and nanofluid stability of MWCNTs in sono heat exchanger: an experimental study, Heat Mass Transf. 58 (3) (2022) 467–479, 03/01, 2022.

[11] Y. Khetib, A.A. Alahmadi, A. Alzaed, H. Azimy, M. Sharifpur, G. Cheraghian, Effect of straight, inclined and curved fins on natural convection and entropy generation of a nanofluid in a square cavity influenced by a magnetic field, Processes 9 (8) (2021) 1339.

[12] H. Azimy, N. Azimy, A.H. Meghdadi Isfahani, S.A. Bagherzadeh, M. Farahnakian, Analysis of thermal performance and ultrasonic wave power variation on heat transfer of heat exchanger in the presence of nanofluid using the artificial neural network: experimental study and model fitting, J. Therm. Anal. Calorim. 148 (16) (2023) 8009–8023, 08/01, 2023.

[13] Y. Peng, M.B. Ghahnaviyeh, M.N. Ahmad, A. Abdollahi, S.A. Bagherzadeh, H. Azimy, A. Mosavi, A. Karimipour, Analysis of the effect of roughness and concentration of Fe3O4/water nanofluid on the boiling heat transfer using the artificial neural network: an experimental and numerical study, Int. J. Therm. Sci. 163 (2021) 106863, 05/01/, 2021.

[14] M.H. Razavi Dehkordi, A.a. Alizadeh, H. Zekri, E. Rasti, M.J. Kholoud, A. Abdollahi, H. Azimy, Experimental study of thermal conductivity coefficient of GNSs-WO3/LP107160 hybrid nanofluid and development of a practical ANN modeling for estimating thermal conductivity, Heliyon 9 (6) (2023) e17539, 06/01/, 2023.

[15] N. Azimy, M.R. Saffarian, Investigation of thermal characteristics and entropy generation in a solar collector including fly ash-Cu hybrid nanofluids: numerical approach using mixture model, Eng. Anal. Bound. Elem. 152 (2023) 169–184, 07/01/, 2023.

[16] M. Hemmat Esfe, S. Alidoust, Modeling and precise prediction of thermophysical attributes of water/EG blend-based CNT nanofluids by NSGA-II using ANN and RSM, Arab. J. Sci. Eng. 46 (7) (2021) 6423–6437, 07/01, 2021.

[17] A. Bin Mahfouz, A. Ali, M. Mubashir, A.S. Hanbazazah, M. Alsaady, P.L. Show, Optimization of viscosity of titania nanotubes ethylene glycol/water-based nanofluids using response surface methodology, Fuel 347 (2023) 128334. /09/01/, 2023.

[18] L. O. Ajuka, M. K. Odunfa, M. O. Oyewola, O. M. Ikumapayi, S. A. Akinlabi, and E. T. Akinlabi, "Modeling of viscosity of composite of TiO2–Al2O3 and ethylene glycol nanofluid by artificial neural network: experimental correlation," Int. J. Interact. Des. Manuf. (IJIDeM), 2022/05/29, 2022.

[19] N. Nayebpashaee, S.M.M. Hadavi, Thermal conductivity and rheological studies for graphene-Al2O3/ethylene glycol-water hybrid nanofluid at low temperatures, Journal of Nano Research 73 (2022) 139–160.

[20] K.M. Yashawantha, A. Asif, G. Ravindra Babu, M.K. Ramis, Rheological behavior and thermal conductivity of graphite–ethylene glycol nanofluid, J. Test. Eval. 49 (4) (2021) 2906–2927.

[21] V. Kumar, A. Pare, A. K. Tiwari, and S. K. Ghosh, "Efficacy evaluation of oxide-MWCNT water hybrid nanofluids: an experimental and artificial neural network approach," Colloids Surf. A Physicochem. Eng. Asp., vol. 620, pp. 126562, 2021/07/05/, 2021.

[22] L. Li, Y. Zhai, Y. Jin, J. Wang, H. Wang, and M. Ma, "Stability, thermal performance and artificial neural network modeling of viscosity and thermal conductivity of Al2O3-ethylene glycol nanofluids," Powder Technol., vol. 363, pp. 360–368, 2020/03/01/, 2020.

[23] A. Akhgar, D. Toghraie, N. Sina, and M. Afrand, "Developing dissimilar artificial neural networks (ANNs) to prediction the thermal conductivity of MWCNT-TiO2/water-ethylene glycol hybrid nanofluid," Powder Technol., vol. 355, pp. 602–610, 2019/10/01/, 2019.

[24] M. Sepehrnia, H. Maleki, M. Karimi, E. Nabati, Examining rheological behavior of CeO2-GO-SA/10W40 ternary hybrid nanofluid based on experiments and COMBI/ANN/RSM modeling, Sci. Rep. 12 (1) (2022) 22054.

[25] A. Shahsavar, M. Sepehrnia, H. Maleki, R. Darabi, Thermal conductivity of hydraulic oil-GO/Fe3O4/TiO2 ternary hybrid nanofluid: experimental study, RSM analysis, and development of optimized GPR model, J. Mol. Liq. 385 (2023) 122338.

[26] M. Sepehrnia, S. Davoodabadi Farahani, A. Hamidi Arani, A. Taghavi, H. Golmohammadi, Laboratory investigation of GO-SA-MWCNTs ternary hybrid

nanoparticles efficacy on dynamic viscosity and wear properties of oil (5W30) and modeling based on machine learning, Sci. Rep. 13 (1) (2023) 10537.
[27] M. Sepehrnia, H. Maleki, M.F. Behbahani, Tribological and rheological properties of novel MoO3-GO-MWCNTs/5W30 ternary hybrid nanolubricant: experimental measurement, development of practical correlation, and artificial intelligence modeling, Powder Technol. 421 (2023) 118389.
[28] A. Afshari, M. Akbari, D. Toghraie, M.E. Yazdi, Experimental investigation of rheological behavior of the hybrid nanofluid of MWCNT–alumina/water (80%)–ethylene-glycol (20%) new correlation and margin of deviation, J. Therm. Anal. Calorim. 132 (2018) 1001–1015.
[29] A. Shahsavar, M. Sepehrnia, A. Fateh Moghaddam, and S. Davoodabadi Farahani, "Effects of sonication time on thermophysical properties of ternary hybrid nanofluid and modeling thermophysical properties utilizing two GMDH and SVR models based on machine learning," J. Taiwan Inst. Chem. Eng., vol. 163, pp. 105650, 2024/10/01/, 2024.
[30] B. Bakthavatchalam, N.B. Shaik, P.B. Hussain, An artificial intelligence approach to predict the Thermophysical properties of MWCNT Nanofluids, Processes 8 (6) (2020) 693.
[31] S. Ihssan, N.B. Shaik, N. Belouaggadia, M. Jammoukh, A. Nasserddine, Enhancing PEHD pipes reliability prediction: integrating ANN and FEM for tensile strength analysis, Applied Surface Science Advances 23 (2024) 100630.
[32] H.A. Umar, N.B. Shaik, M. Inayat, S.A. Sulaiman, ANN-RSM based multi-parametric optimisation and modelling of H2 and syngas from co-gasification of residues from oil palm plants, Process. Saf. Environ. Prot. 188 (2024) 759–780.
[33] N.B. Shaik, K. Jongkittinarukorn, W. Benjapolakul, K. Bingi, A novel neural network-based framework to estimate oil and gas pipelines life with missing input parameters, Sci. Rep. 14 (1) (2024) 4511.
[34] A.R. Abbasian, M.H.R. Dehkordi, N. Azimy, H. Azimy, M. Akbari, B. Ayadi, W. Aich, L. Kolsi, Experimental study of preparing the CoFe2O4 magnetic nanofluid and measuring thermal-fluid characteristics of the stabilized magnetocaloric nanofluid, Mater. Sci. Eng. B 306 (2024) 117462.